www.czasopisma.pan.pl PAN www.journals.pan.pl

ARCHIVES of FOUNDRY ENGINEERING

ISSN (2299-2944)
Volume 21
Issue 1/2021

11 – 17

2/1

10.24425/afe.2021.136072

Published quarterly as the organ of the Foundry Commission of the Polish Academy of Sciences

Aluminium Loss During Ti-Al-X Alloy Smelting Using the VIM Technology

A. Smalcerz*, L. Blacha, J. Łabaj
Silesian University of Technology, Faculty of Materials Engineering and Metallurgy
ul. Krasińskiego 8, 40-019 Katowice, Poland
* Corresponding author. E-mail address: albert.smalcerz@polsl.pl

Received 22.04.2020; accepted in revised form 13.07.2020

Abstract

Titanium alloys belonging to the group of modern metallic materials used in many industries, including the aerospace industries. Induction crucible vacuum furnaces and induction furnaces with cold crucible are most commonly used for their smelting. When operating these devices, one can deal with an adverse phenomenon of decrease in the content of alloy elements that are characterized by higher equilibrium vapour pressure than the matrix metal or titanium, in the metal bath. In the paper, results of the study on aluminium evaporation from the Ti-Al-Nb, Ti-Al-V and Ti-Al alloys (max 6.2 % wt.) during smelting in a vacuum induction melting (VIM) furnace are presented. The experiments were performed at 10 to 1000 Pa for 1973 K and 2023 K. A significant degree of aluminium loss has been demonstrated during the analysed process. The values of relative aluminium loss for all the alloys ranged from 4 % to 25 %. Lowering the pressure in the melting system from 1000 Pa to 10 Pa resulted in increased values of aluminium evaporation flux from $4.82 \cdot 10^{-5}$ to 0.000327 $g \cdot cm^{-2} \cdot s^{-1}$ for 1973 K and from $9.28 \cdot 10^{-5}$ to 0.000344 $g \cdot cm^{-2} \cdot s^{-1}$ for 2023 K. The analysis of the results obtained took into account the value of the actual surface of the liquid metal. In the case of melting metals in an induction furnace, this surface depends on the value of power emitted in the charge. At greater power, we observe a significant increase in the bath surface due to the formation of a meniscus.

Keywords: Melting of Ti-Al alloys, Induction vacuum furnace, Evaporation of metals

1. Introduction

Rapid advancements in technology, observed over the recent years, have mostly resulted from improvements in production technologies of various types of metallic, ceramic and composite materials with unique properties. Such materials are e.g. metal alloys based on intermetallic Fe-Al phases, nickel-based superalloys or titanium alloys. The last mentioned, due to their small specific densities, high corrosion resistance or high-temperature strength, are applied in e.g. aerospace, defence and automotive industries. Among titanium-based materials, the most commonly used types are Ti-Al-X alloys. However, their production technologies are associated with many difficulties due to three factors: a high smelting temperature, high reactivity of titanium with the crucible materials and a potential for evaporation of the alloy components with higher vapour pressures than that of the metal matrix during the smelting process [1-11]. To avoid the problem of titanium reactivity with crucible materials, cold crucible furnaces are increasingly being used. In this type of furnaces, crucible is usually made of water-cooled copper segments. The electro-dynamic interaction between the currents induced in the crucible and the charge causes the liquid metal to be pushed away from the walls of the crucible, and the charge only contacts its base.. The problem of metal bath component loss during production of a specific alloy is particularly important when even a small change of their contents leads to altered alloy properties. In the present paper, aluminium evaporation from the Ti-Al-Nb, Ti-Al-V and Ti-Al alloys during

smelting in a crucible vacuum induction melting furnace has been discussed.

2. Research methodology

The research experiments were performed on multi-component alloys; their composition is presented in Table 1.

Table 1.
Chemical composition of the investigated alloy

Type of alloy	Content of basic alloy components, wt. %			
	Al	Nb	V	Ti
Ti-Al-Nb	4.15	7.5	0.034	residue
Ti-Al-V	5.5	-	3.70	residue
Ti-Al	6.2	-	-	residue

The melting system applied in the experiments was a SecoWarwick VIM-20 vacuum induction melting furnace; its image is presented in Fig. 1.

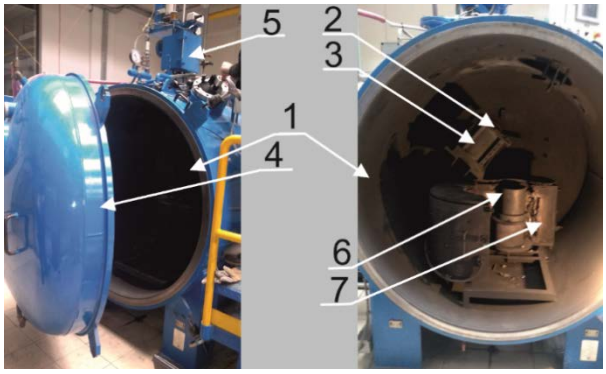

Fig. 1. The Seco-Warwick VIM-20 vacuum induction melting furnace: 1 – the furnace chamber, 2 – the crucible, 3 – the induction coil, 4 – the door to close the chamber tightly, 5 – the measurement system, 6 – the ingot mould, 7 – the ingot mould heater

This furnace type selection resulted from its being a device widely used for titanium alloy smelting. At the beginning of each experiment, an alloy sample (about 1000 g) was placed in a graphite crucible located inside the induction coil of the furnace. When the furnace chamber was closed, a precisely specified vacuum was generated using diffusive and Roots pumps. After stabilisation of the chamber pressure, the crucible was heated up to the set temperature. During each experiment, metal specimens were collected and analysed for the aluminium content. The experiments were performed at 10 to 1000 Pa for 1973 K and 2023 K.

2.1. Composition of the gaseous phase over liquid Ti-Al-X alloys

To determine the equilibrium composition of the gaseous phase over the investigated alloys, the thermodynamic database HSC Chemistry ver. 6.1 was used [12]. Estimated values of the equilibrium vapour pressure for Ti, Al, V and Nb over pure components are listed in Table 2, and the vapour pressures of these metals over the analysed alloys – in Table 3. They were determined based on the thermodynamic data regarding activity coefficients of the individual components of the analysed liquid titanium alloys included in the papers by Semiatin, Song, Zhu and Belyanchikov [13-16]. Fig. 2 shows ratios of the titanium vapour pressures to the aluminium values over these alloys. The data in Fig. 2 demonstrate that for the range of 1923 K to 2173 K, the ratio is 0.01 to 0.05. This means the aluminium equilibrium pressures significantly exceed those for titanium and, therefore, there is a potential for intense evaporation of this component of the investigated alloys during smelting, from the thermodynamic point of view.

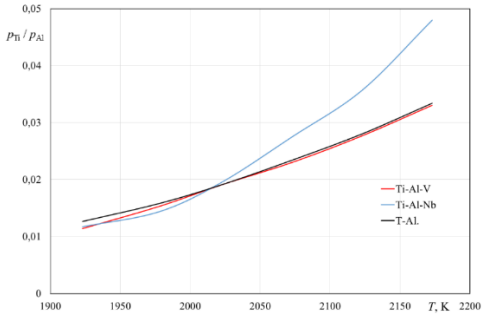

Fig. 2. Effects of temperature on the p_{Ti} / p_{Al} value

Table 2.
Determined p_i^o values for titanium, aluminum, vanadium and niobium

Alloy component	p_i^o, Pa					
	1923 K	1973 K	2023 K	2073 K	2123 K	2173 K
Titanium	0.34	0.68	1.33	2.49	4.52	7.96
Aluminium	289.4	468.1	738.8	1139.75	1721.4	2549.2
Vanadium	0.05	0.12	0.26	0.53	1.06	2.04
Niobium	$5.41 \cdot 10^{-8}$	$1.76 \cdot 10^{-7}$	$5.41 \cdot 10^{-7}$	$1.57 \cdot 10^{-6}$	$4.34 \cdot 10^{-6}$	$9.06 \cdot 10^{-6}$

Table 3.
Determined vapour pressure values for titanium, aluminum, vanadium and niobium over the liquid alloys Ti-Al-V, Ti-Al-Nb and Ti-Al

	p_i^o, Pa					
	1923 K	1978 K	2023 K	2073 K	2123 K	2173 K
Type of alloy	Ti-Al-V					
Titanium	0.07	0.16	0.33	0.64	1.21	2.22
Aluminum	6.15	10.46	17.27	27.81	43.71	67.19
Vanadium	0.001	0.003	0.007	0.013	0.026	0.053
Type of alloy	Ti-Al-Nb					
Titanium	0.07	0.14	0.30	0.63	1.19	2.09
Aluminum	5.98	9.75	15.32	18.90	33.34	43.56
Niobium	$2.3 \cdot 10^{-10}$	$8.4 \cdot 10^{-10}$	$3.3 \cdot 10^{-9}$	$8.7 \cdot 10^{-9}$	$4.1 \cdot 10^{-8}$	$1.1 \cdot 10^{-7}$
Type of alloy	Ti-Al					
Titanium	0.08	0.17	0.34	0.67	1.26	2.31
Aluminum	6.33	10.76	17.78	28.62	44.97	69.17

3. Experimental results and discussion

Overall results of all experimental melting processes for the Ti-Al-Nb, Ti-Al-V and Ti-Al alloys are summarised in Table 4. In addition to the experimental parameters, it contains the values of final aluminium content in the alloy, relative loss of this metal from the alloy and the aluminium evaporation flux.

Table 4.
Results of vacuum melting experiments for the Ti-Al-Nb, Ti-Al-V and Ti-Al alloys

Type of alloy	T, K	p, Pa	Aluminium final concentration, % mas.	U_{BAl}, %	N_{Al} g cm^{-2}s^{-1}
Ti-Al-Nb	2023	10	3.48	16.14458	0.000170
Ti-Al-Nb	2023	50	3.58	13.73494	0.000144
Ti-Al-Nb	2023	100	3.63	12.53012	0.000131
Ti-Al-Nb	2023	1000	3.79	8.674699	$9.28e^{-05}$
Ti-Al-Nb	1973	10	3.66	11.80723	0.000124
Ti-Al-Nb	1973	50	3.72	10.36145	0.000109
Ti-Al-Nb	1973	100	3.77	9.156627	$9.64e^{-05}$
Ti-Al-Nb	1973	1000	3.96	4.578313	$4.82e^{-05}$
Ti-Al-V	2023	10	4.10	25.45455	0.000344
Ti-Al-V	2023	50	4.24	22.90909	0.00031
Ti-Al-V	2023	100	4.33	21.27273	0.000259
Ti-Al-V	2023	1000	4.48	18.54545	0.000189
Ti-Al-V	1973	10	4.17	24.18182	0.000327
Ti-Al-V	1973	50	4.27	22.36364	0.000303
Ti-Al-V	1973	100	4.36	20.72727	0.00028
Ti-Al-V	1973	1000	4.72	14.18182	0.000192
Ti-Al	2023	10	5.35	17.69231	0.000306
Ti-Al	2023	50	5.61	13.69231	0.000237
Ti-Al	2023	100	5.67	12.76923	0.000221
Ti-Al	2023	1000	5.82	10.46154	0.000181
Ti-Al	1973	10	5.58	14.15385	0.000245
Ti-Al	1973	50	5.65	13.07692	0.000226
Ti-Al	1973	100	5.70	12.30769	0.000213
Ti-Al	1973	1000	5.83	10.30769	0.000178

The Table 4 data show that the determined aluminium loss for all tested alloys increased as the operating pressure of the melting system decreased, and ranged from 4 % to 25 %. By analogy, the vacuum increase (1000 to 10 Pa) caused higher aluminium evaporation flux values.

While analysing the process of aluminium evaporation from liquid titanium alloys during their smelting in the vacuum

induction melting furnace, three factors that may affect the rate of this process should be mentioned: the operating pressure in the melting system, the metal bath surface area and its stirring rate. There are four pressure ranges to alternately affect the evaporation process discussed [17-21]. The first range is related to pressures that cause the metal evaporation rate to reach its maximum which remains stable as the pressure further decreases. So-called free evaporation is observed at that time during which the evaporating metal atoms or molecules that are leaving the metal bath surface do not collide with other gaseous molecules so their velocity is the same as it was while leaving this surface. The other pressure range concerns the values for which the process rate is practically controlled only by mass transfer processes in the liquid phase. When the pressure in the system is raised above this value, a change of the stage that determines the analysed process is observed. This refers to pressures of up to several hundred Pa. Within this pressure range, the evaporation rate is determined by mass transfer processes in both the gaseous and liquid phases. For higher pressures, diffusion control is present and the process rate is determined exclusively by the mass transfer in the gaseous phase. Such a process control is usually seen for pressures above 1000 Pa.

The value of evaporation flux of the liquid alloy component is directly proportional to the evaporation surface area i.e. the metal bath surface in the analysed case which, for the induction furnace, increases with higher power values. The higher power results in a considerably larger bath surface area due to meniscus formation which is the effect of electromagnetic field influencing the liquid metal. It is illustrated in Fig. 3 in images of the surface of aluminium melted in the experimental system.

a)

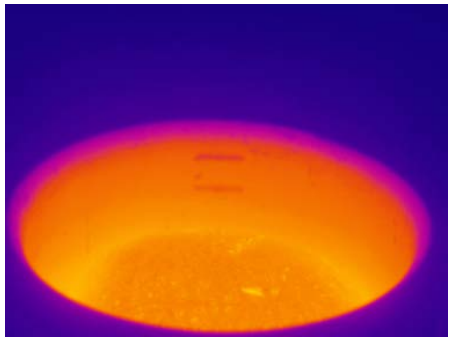

b)

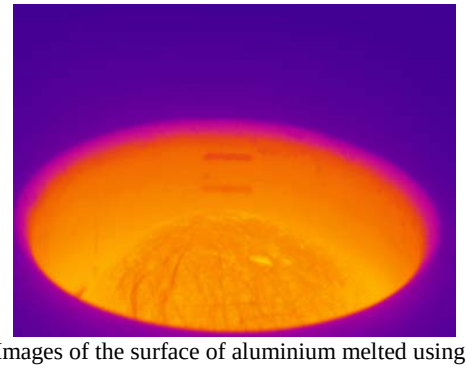

Fig. 3. Images of the surface of aluminium melted using various furnace operating power values: a) 11 kW; b) 37 kW

Simulations related to the effects of the operating electrical parameters of the induction furnace showed that increasing frequencies of the induction coil-supplying current were associated with higher mean bath stirring rates within the whole liquid metal volume as well as with higher near-surface rates [22]. In addition, these values depend on the position of the crucible versus the induction coil. While changing the crucible location inside the induction coil, we alter the electromagnetic field distribution and, thus, the bath stirring rate, which is observed at the metal surface in particular. Greater distances of the lower bath surface from the lower induction coil edge (the crucible is not symmetrically placed against the induction coil) result in smaller stirring rates of the metal [23]. Increased stirring rates may cause intensified evaporation during melting processes performed at the vacuum of less than several Pa.

The paper [24] presents results of a mathematical simulation allowing determination of the liquid titanium surface area and the mean bath stirring rate for the system used in the experiments discussed in this paper. To determine the velocity field, a model of coupled electromagnetic and hydrodynamic fields of liquid metal was applied. It should be noted that an essential problem that impedes modelling of this process is the fact that the electromagnetic field affects the hydrodynamic field of liquid metal bath, while changing its surface shape. Due to the shape changes that cause electromagnetic field distribution alterations, it is necessary to calculate the electromagnetic and hydrodynamic fields at each simulation step [25, 26] or with a frequency sufficient for maintaining the current field distribution by means of the mathematical extrapolation [27, 28].

The numerically determined shape of the liquid titanium surface for the following model parameters is presented in Fig. 4: current intensity 738 A, current frequency 5 kHz, titanium resistivity (metal) $1.7e^{-6}$ Ω·m, graphite resistivity (crucible) 10 Ω·m and copper resistivity (induction coil) 0.018 Ω·m.

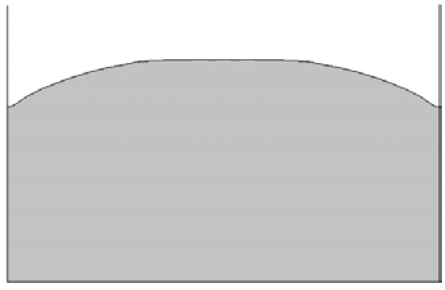

Fig. 4. Titanium bath shape in the presence of electromagnetic field (T=2173 K) [24]

The liquid titanium velocity field for the same melting system is presented in Fig. 5. The results of simulations performed for both the meniscus size and the stirring rate of liquid titanium are summarised in Table 5.

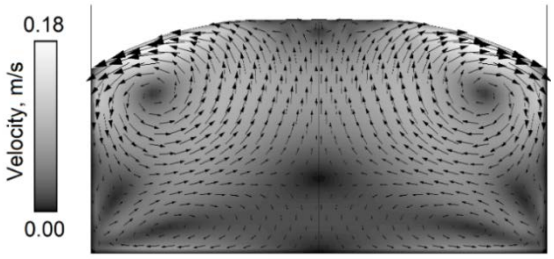

Fig. 5. Liquid titanium velocity field [24]

Table 5.
Results of the simulations for both the velocity field and the surface area of liquid titanium melted in the VIM-20 furnace at 2173 K

Maximum EM force	52.9 kN
Mean EM force	11.7 kN
Maximum titanium volumetric velocity	0.18 m/s
Mean titanium volumetric velocity	0.06 m/s
Titanium free surface area (meniscus)	0.0068 m^2
Surface area of the crucible cross-section	0.0060 m^2
Maximum titanium surface velocity	0.185 m/s
Mean titanium surface velocity	0.135 m/s

Figs. 6 and 7 present the experiment-determined relationships between relative aluminum loss from the Ti-Al-Nb, Ti-Al-V alloys and the operating pressure in the melting system. The parameter value for all the alloys ranged from 4 % to 25 %.

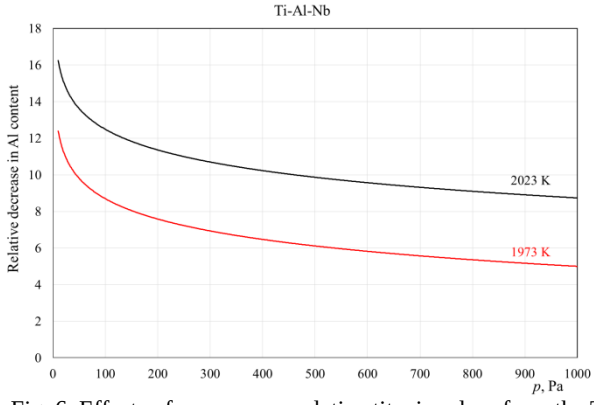

Fig. 6. Effects of pressure on relative titanium loss from the Ti-Al-Nb alloy

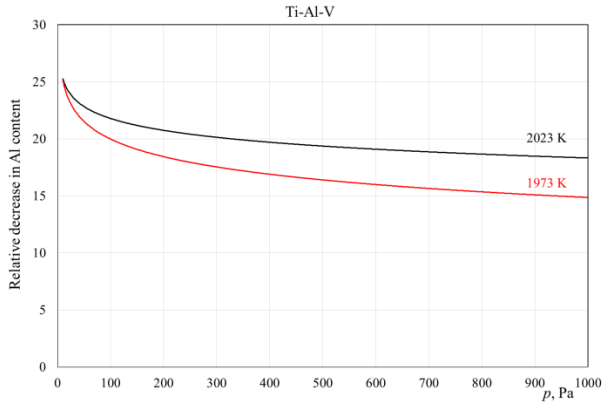

Fig. 7. Effects of pressure on relative titanium loss from the Ti-Al-V alloy

The experiment-determined relationships between the aluminium evaporation flux and the operating pressure in the melting system for the investigated Ti-Al-Nb and Ti-Al-V alloys are shown in Figs. 8 and 9.

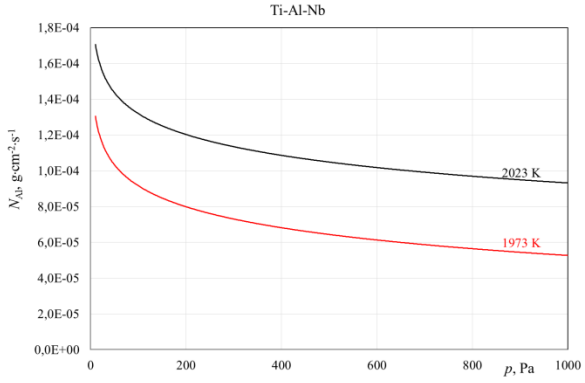

Fig. 8. Effects of the operating pressure in the induction furnace on the aluminium evaporation flux from the Ti-Al-Nb alloy

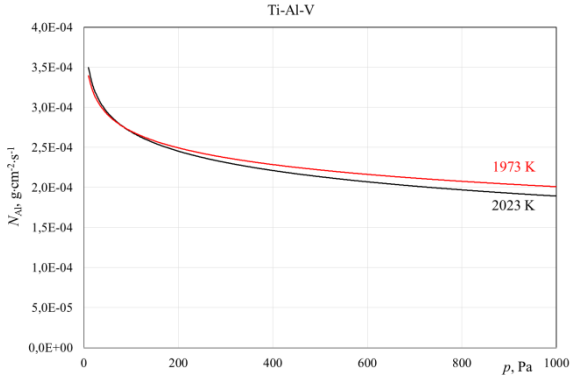

Fig. 9. Effects of the operating pressure in the induction furnace on the aluminium evaporation flux from the Ti-Al-V alloy

Figure 10 presents determined conventional pressure ranges for both intense and minimum aluminium evaporation from the investigated alloys. These curves were plotted based on

relationships proposed in the paper [11] where the authors demonstrated that for multi-component titanium alloys containing up to 23 % wt. Al, the value of allowable pressure pall could be determined as follows:

$$p_{all} = 5.5 \cdot p_{Al} \quad (1)$$

while the critical pressure:

$$p_{cri} = 0.55 \cdot p_{Al} \quad (2)$$

where: p_{Al} – equilibrium pressure of Al over the alloy.

The range above the line pall corresponds to the pressure at which aluminium evaporation is negligible while the range below the line p_{cri} corresponds to the pressures at which significant aluminium loss during Ti-Al melting processes in vacuum induction melting furnaces is observed.

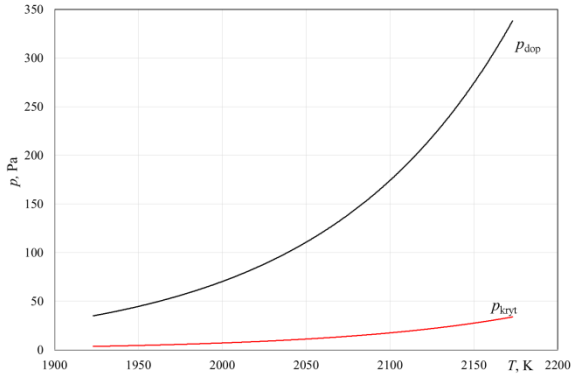

Fig. 10. Effects of melting temperature on the pall and pcri parameters for the investigated Ti-Al-X alloys

3. Summary

The results of investigations regarding Ti-Al-Nb, Ti-Al-V and Ti-Al (max 6.2 % wt. Al) alloy smelting in the vacuum induction melting furnace at 10 to 1000 Pa (operating pressure) for 1973 K an 2023 K showed a significant aluminum loss during the analysed process. Relative aluminum loss values for all the alloys ranged from 4 % to 2 5%. Lowering the pressure from 1000 Pa to 10 Pa in the melting system resulted in increased values of the aluminum evaporation flux from $4.82 \cdot 10^{-5}$ to 0.000327 $gcm^{-2}s^{-1}$ for 1973 K and from $9.28 \cdot 10^{-5}$ to 0.000344 $gcm^{-2}s^{-1}$ for 2023 K. The estimated values of hypothetical allowable and critical pressures for the alloys containing approx. 6 % wt. Al were, respectively, 57 Pa and 5 Pa for 1973 K as well as 95 Pa and 10 Pa for 2023 K. It means that in order to limit the undesirable effect of aluminum evaporation from the investigated alloys, the smelting process should be performed at the operating pressure not higher than 60 Pa for 1973 K and 100 Pa for 2023 K.

Acknowledgement

This study is part of the 11/990/BK_20/0074 funded by Silesian University of Technology.

References

[1] Kostov, A. & Friedrich, B. (2005). Selection of crucible oxides in molten titanium and titanium aluminium alloys by thermo-chemistry calculation. *Journal of Mining and Metallurgy*. 41B, 113-125. DOI: 10.2298/JMMB0501113K.
[2] Kuang, J.P., Harding, R.A. & Campbell, J. (2000). Investigation into refractories as crucible and mould materials for melting and casting gamma-TiAl alloys. *Materials Science and Technology*. 16, 1007-1016. DOI.org/10.1179/026708300101508964.
[3] Tetsui, T., Kobayashi, T., Mori, T., Kishimoto, T. & Harada, H. (2010). Evaluation of yttrium applicability as a crucible for induction melting of TiAl alloy. *Materials Transactions*. 51, 1656-1662. DOI:10.2320/matertrans.MAW20100.
[4] Myszka, D., Karwiński, A., Leśniewski, W. & Wieliczko, P. (2007). Influence of the type of ceramic moulding materials on the top layer of titanium precision castings. *Archives of Foundry Engineering*. 7(1), 153-156. DOI: 10.7356/iod.2015.24.
[5] Szkliniarz, A. & Szkliniarz, W. (2011). Assessment quality of Ti alloys melted in induction furnace with ceramic crucible. *Solid State Phenomena*. 176, 139-148. DOI: 10.4028/www.scientific.net/SSP.176.139
[6] Jinjie, G., Jun, J., Yuan, S.L., Guizhong, L., Yanqing, S. & Hongsheng, D. (2000). Evaporation behavior of aluminum during the cold crucible induction skull melting of titanium aluminum alloys. *Metallurgical and Materials Transactions B*. 31B, 837-844. DOI.org/10.1007/s11663-000-0120-1.
[7] Isawa, T., Nakamura, H. & Murakami, K. (1992). Aluminum evaporation from titanium alloys in EB hearth melting. *ISIJ International*. 32, 607-615.
[8] Ivanchenko, V., Ivasishin, G. & Semiatin, S. (2003). Evaluation of evaporation losses during electron-beam melting of Ti-Al-V alloys. *Metallurgical and Materials Transactions B*. 34B, 911-915. DOI: 10.1007/s11663-003-0097-7.
[9] Su, Y., Guo, J., Jia, J., Liu, G. & Liu, Y. (2002). Composition control of a TiAl melt during the induction skull melting (ISM) process. *Journal of Alloys and Compounds*. 334, 261-266. DOI: 10.1016/S0925-8388(01)01766-2.
[10] Guo, J., Liu, G., Su, Y., Ding, H., Jia, J. & Fu, H. (2002). The critical pressure and impeding pressure of Al evaporation during induction skull melting processing of TiAl. *Metallurgical and Materials Transactions A*. 31A, 3249-3253. DOI.org/10.1007/s11661-002-0311-2.
[11] Gou, J., Liu, Y., Su, Y., Ding, H., Liu, G. & Jia, J. (2000). Evaporation behaviour of aluminum during the cold crucible induction skull melting of titanium aluminum alloys. *Metallurgical and Materials Transactions B*. 31B, 837-844. DOI.org/10.1007/s11663-000-0120-1.

[12] HSC Chemistry ver. 6.1. Outocumpu Research Oy, Pori.
[13] Semiatin, S., Ivanchenko, V., Akhonin, S.O. & Ivasishin, O.M. (2004). Diffusion models for evaporation losses during electron-beam melting of alpha/beta-titanium alloys. *Metallurgical and Materials Transactions B.* 35B, 235-245. DOI.org/10.1007/s11663-004-0025-5.
[14] Song, J.H., Min, B.T., Kim, J. H., Kim, H.W., Hong, S.W. & Chung, S.H. (2005). An electromagnetic and thermal analysis of a cold crucible melting. *International Communications in Heat and Mass Transfer*. 32, 1325-1336. DOI.org/10.1016/j.icheatmasstransfer.2005.07.015.
[15] Zhu, Y., Yang, Y.Q. & Sun, J. (2004). Calculation of activity coefficients for components in ternary Ti alloys and intermetallics as matrix of composites. *Transactions of Nonferrous Metals Society of China*. 14, 875-879.
[16] Belyanchikov, L.N. (2010). Thermodynamics of Titanium-Based Melts: I. Thermodynamics of the Dissolution of Elements in Liquid Titanium. *Russian Metallurgy*. 6, 565-567. DOI.org/10.1134/S0036029510060194.
[17] Blacha, L. & Labaj, J. (2012). Factors determining the rate of the process of metal bath components. *Metalurgija*. 51, 529-533.
[18] Ward, R.G. (1963). Evaporative losses during vacuum induction melting of steel. *Journal of the Iron and Steel Institute*. 1, 11-15.
[19] Labaj, J. (2010). *Copper evaporation kinetics from liquid iron*. Wydawnictwo Oldprint. (in Polish).
[20] Ozberk, E. & Guthrie, R. (1985). Evaluation of vacuum induction melting for copper refining. *Transactions of the Institution of Mining and Metallurgy, Section C: Mineral Processing and Extractive Metallurgy*. 94, 146-157.
[21] Ozberk, E. & Guthrie, R. (1986). A kinetic model for the vacuum refining of inductively stirred copper melts. *Metallurgical Transactions B.* 17, 87-103.
[22] Przyłucki, R., Golak, S., Oleksiak, B. & Blacha, L. (2012). Influence of an induction furnace's electric parameters on mass transfer velocity In the liquid phase. *Metalurgija*. 1, 67-70.
[23] Blacha, L., Przylucki, R., Golak, S. & Oleksiak, B. (2011). Influence of the geometry of the arrangement inductor - crucible to the velocity of the transport of mass in the liquid metallic phase mixed inductive. *Archives of Civil and Mechanical Engineering*. 11, 171-179. DOI: 10.1016/S1644-9665(12)60181-2.
[24] Blacha, L., Golak, S., Jakovics, S. & Tucs, A. (2014). Kinetic analysis of aluminum evaporation from Ti-6Al-7Nb. *Archives of Metallurgy and Materials*. 59, 275-279. DOI: 0.2478/amm-2014-0045
[25] Spitans, S., Jakovics, A., Baake, E. & Nacke, B. (2010). Numerical modelling of free surface dynamics of conductive melt in the induction crucible furnace. *Magnetohydrodynamics*. 46, 425-436
[26] Spitans, S., Jakovics, A., Baake, E. & Nacke, B. (2011). Numerical modelling of free surface dynamics of melt in an alternate electromagnetic field. *Magnetohydrodynamics*. 47, 385-397.
[27] Golak, S. & Przylucki, R. (2008). The optimization of an inductorposition for minimization of a liquid metal free surface, *Przeglad Elektrotechniczny*. 84, 163-164.
[28] Golak, S. & Przyłucki R. (2009). A simulation of the coupled problem of magnetohydrodynamics and a free surface for liquid metals. WIT *Transactions of Engineering Science*. 48, 67-76. DOI: 10.2495/MPF090061.